Analytical transport model of AlGaN/GaN HEMT based on electrical and thermal measurement

J-C Jacquet[1], R. Aubry[1], H. Gérard[2], E. Delos[2], N. Rolland[2], Y. Cordier [3], A. Bussutil[1], M. Rousseau[2] and S. L. Delage[1]

TIGER : Common Laboratory TRT – IEMN
[1]: TRT Domaine de Corbeville 91404 Orsay Cedex/France
[2]: IEMN Avenue Poincaré 59652 Villeneuve d'Ascq.
[3]:CRHEA -CNRS, rue Bernard Gregory, 06560 Valbonne, France

ABSTRACT — **GaN and its related alloys constitute a family of wide bandgap semiconductors suitable to optoelectronics and power microwave applications. For the latter applications, their high breakdown fields in the 3MV/cm range and their high peak electron velocity above 10^7cm/s are crucial. The high electron mobility transistor (HEMT) based on GaN is suitable to high frequencies and power applications. Moreover, those materials show excellent chemical and metallurgical stability. One peculiarity of GaN is stemming from the fact that the crystal growth is mostly achieved by heteroepitaxy since no commercial GaN substrates are yet available. The substrates currently chosen are sapphire, silicon carbide and silicon. The high power RF device performance decreases as operation temperature increases (e.g. fall of electron mobility impacting the cut-off frequencies and degradation of device reliability) so it is very important to understand the thermal effect in the device. This work present an analytical model of electron transport based on, at one hand, experimental characterisation such as I-V pulsed measurement, thermal characterisation and, at the other hand, thermal simulation and physical analysis. We were able to derive the variation of the electron velocity model as a function of temperature thanks to the thermal characterisation of parameters such electron mobility, ohmic contact, carrier density and gate Schottky barrier.**

I. INTRODUCTION

The component used to derive the analytical model was an AlGaN/GaN HEMT grown on silicon.

Materials: The $Al_{0.3}Ga_{0.7}N$/GaN structure was grown on Si by molecular beam epitaxy. The epitaxial structure consists of: 1nm GaN/30nm $Al_{0.3}Ga_{0.7}N$/1.5µm GaN (nid)/520nm AlN/280µm Si(111). The Hall effect measurements showed a sheet carrier density of $9x10^{12}$ cm^{-2} and a 2-D gas mobility of about 1000 $cm^2V^{-1}s^{-1}$ at room temperature.

Device: Ti/Al layers were evaporated and annealed to obtain good ohmic contacts Pt/Au gates with 0.8µm footprint were defined by electron beam lithography and the devices were passivated with Si_3N_4 deposited by plasma enhanced chemical vapour deposition.

II. MATERIAL AND TECHNOLOGICAL THERMAL ASSESMENT

In order to carry out a precise thermal analysis, Hall measurements were realised as a function of temperature. The figure 1.a. shows the 2-D gas electron mobility from 100K to 500K. The figure 1.b. shows the sheet carrier density n_s within the same temperature range. n_s is almost constant up to 400K, and a slight increase is observed and this was attributed to surface charge variation, e.g. trap ionisation. The figure 2 shows the variation of the access resistance R_C between 290°C to 520°C.A steady increase was observed from 0.6 Ωmm to 1.25 Ωmm. C-V measurement were also carried out on 100x100µm² Schottky diodes to extract the barrier height as a function of temperature. A non-expected increase of the barrier height was observed from 0.8eV to 1.25eV.

III. DETERMINATION OF THE CHANNEL TEMPERATURE

Two-finger transistors were used for the thermal assessment. Each gate had a width of 250 µm with a 3µm source-drain contact spacing. The finger pitch was kept constant at 35 µm. The diced devices were then brazed on a gold plated 200µm thick copper plate before characterisation. A new I-V bench was recently developed, which is allowing close to perfect 100ns pulsed DC measurements of devices. The equipment was also including a hot plate and a regulator to control the device temperature.

The AlGaN/GaN HEMTs channel temperature was determined by the mean of I-V characteristics in DC and under 100ns pulsed conditions as a function of chuck temperature. We measured the device dynamic characteristics by pulsing simultaneously the drain and the gate. A small duty cycle of 0.1% was used to limit the chance of "thermal memory effect" between each individual pulse. The idle point was fixed at V_{GS} and V_{DS} both equals to 0V to leave the traps at an occupation level quasi-constant due to their long time response.

The innovative approach of our work is stemming from the study of the device self-heating as a

function of the pulse duration. Classically only the shortest pulses are used to determine the DC channel temperature. However by analysing the temperature measured for different time constant using a gauge signal fixed at 100ns, we were able "to map" the thermal resistance along the depth of the component**.** By plotting the channel temperature as a function of the dissipated power, like on figure 5, we calculated the thermal resistance and found a value near of 40 °CW^{-1} after 1 ms. We could not measure directly the temperature increase at the device turn-on from 0s to 100ns. For pulse longer than 1ms a mild current collapse was observed attributed to the presence of traps.

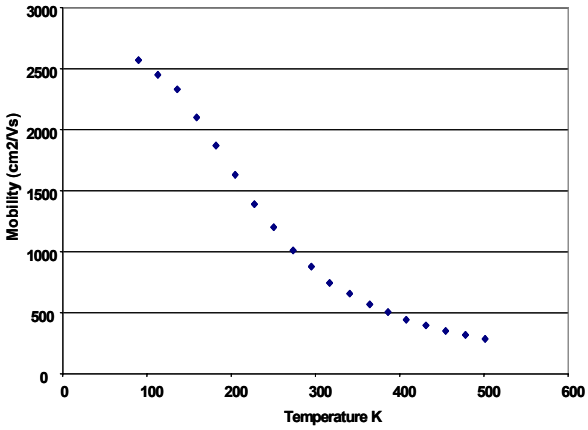

Fig. 1. 2D gas electron mobility from 100 K to 500 K

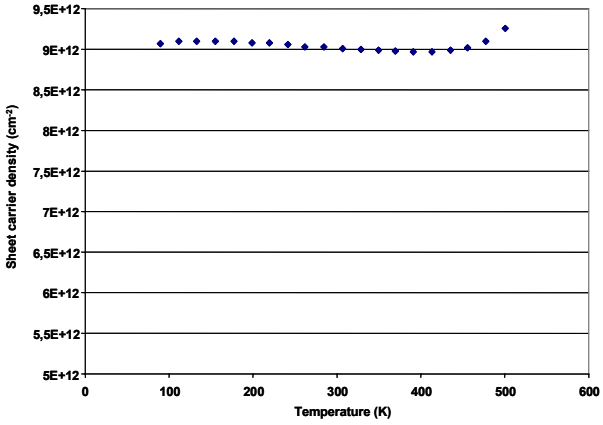

Fig. 2. Sheet carrier density n_s from 100 K to 500 K

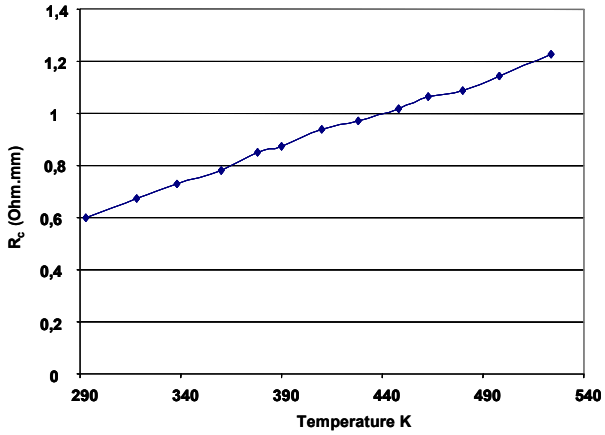

Fig. 3. Access resistance variation from 290 K to 520 K

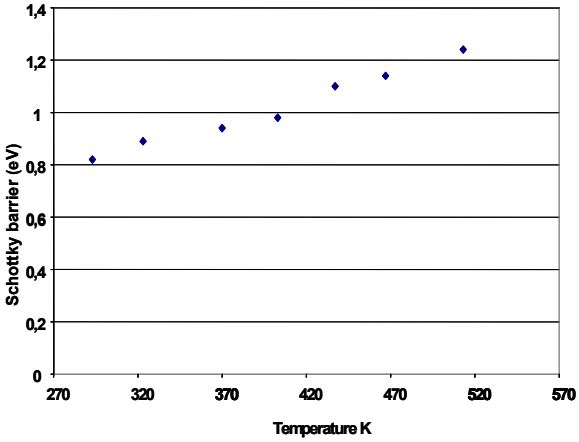

Fig. 4. Schottky barrier height as a function of temperature

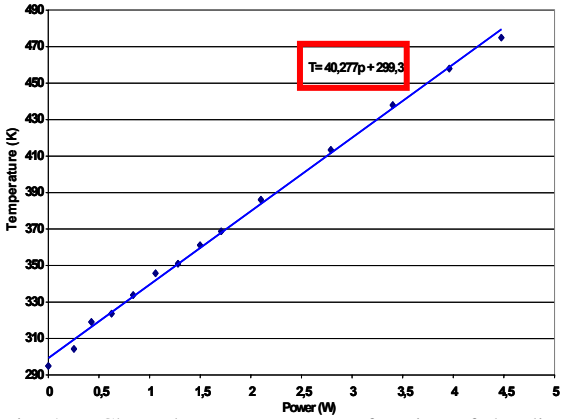

Fig. 5. Channel temperature as a function of the dissipated power from 100 ns to 1ms, the slope is 40°C/W.

Finite element thermal simulations (ANSYS) were realised in the mean time. We found a thermal resistance of 10°C/W between 0 to 100ns and 47°C/W from 0 to 1ms. This means that an incremental thermal resistance of 37°C/W is involved between 100ns to 1ms. This value is therefore very close to the experimental one of 40 we measured experimentally.

IV. ANALYTICAL MODEL

From the thermal dependence of the saturation current, Schottky potential, sheet carrier density, mobility at low field and ohmic contacts we can estimate the saturation velocity and its thermal dependence.

In order to obtain an analytical expression for the saturation current Id_{sat} we need the velocity-field relationship. Many theoretical [1-5] and experimental [6] works predicted for bulk GaN material the existence of a peak velocity of 3 10^7 cm/s for a range of electric fields between 100 to 200 kV/cm and a saturation around 2 10^7 cm/s at higher fields. Although theoretical works predicted also velocity overshoot for 2DEG in GaN-AlGaN heterostructures [7], it is not obvious that these results are in agreement with the real world. Indeed, overshoot effects are originating from two physical effects. The first one is a real space transfer of electrons from the GaN channel into the AlGaN layer. The second one is the transition between high 2D mobility to lower

3D mobility in the GaN layer [7-8]. Nevertheless the gap energy between and satellite valley is bigger to both AlGaN/GaN conduction band offset energy and to energy confinement of electrons in the GaN layer. This could conduct to a transfer of electrons before they experience a velocity overshoot. Moreover hot-phonons effects were predicted and reported to reduce significantly the saturation velocity [9-10]. Experimental results made at 77K show that electron velocity saturate at 10^7 cm/s at a field below 10 kV/cm [8]. For these reasons and in order to determine an analytical expression for Id_{sat} we choose a Si-like velocity-field relationships [11-12]:

$$v[F,T] = \mu_0[T]F/(1+\mu_0[T]F/v_{sat}[T]) \quad (1)$$

$$\mu_0[T] = \mu_0(T/300)^{-1.8} \quad (2)$$

Thermal dependency for v_{sat} is taken to be of the form [13]:

$$v_{sat}[T] = v_{sat}[300]/(1-A+AT/300) \quad (3)$$

Simple charge control model were used [14] and extrinsic saturation current expression (5) is obtained from the second order equation:

$$Id_{sat}[T] = \frac{\varepsilon}{2}\frac{z_g l_g}{d_g}\frac{v_{sat}^2}{\mu_0}\left[\sqrt{1+2\mu_0\times\frac{(V_{gs}^{ext}-V_{th}-R_{ac}Id_{sat})}{l_g v_{sat}}}-1\right]^2 \quad (4)$$

$$Id_{sat}[T] = \varepsilon\frac{z_g}{d_g}\frac{\mu_0}{l_g}\frac{n_s[T]}{n_{s300}}\frac{\left[1+\frac{\mu_0}{l_g v_{sat}}\times(1+\frac{n_s[T]}{n_{s300}}\varepsilon\frac{z_g}{d_g}v_{sat}R_{ac})\times(V_{gs}^{ext}-V_{th})-\sqrt{1+2\frac{\mu_0}{l_g v_{sat}}\times(1+\frac{n_s[T]}{n_{s300}}\varepsilon\frac{z_g}{d_g}v_{sat}R_{ac})\times(V_{gs}^{ext}-V_{th})}\right]}{(\frac{\mu_0}{l_g v_{sat}}\times(1+\frac{n_s[T]}{n_{s300}}\varepsilon\frac{z_g}{d_g}v_{sat}R_{ac}))^2} \quad (5)$$

$$R_{ac}[T] = R_c[T]+\frac{1}{q}\frac{d_{sg}}{z_g}\frac{1}{n_s[T]\mu_0[T]} \quad (6)$$

In these expressions R_{ac}, v_{sat}, μ_0, n_s, V_{th}, R_c are temperature dependent, R_{ac} is the total access resistance (source contact and channel), R_c is the contact resistance, d_{sg} is the gate-source distance, z_g is the gate width, l_g is the gate length, d_g is the mean distance of the 2DEG from the Schottky contact, V_{th} is the pinch-off voltage,

The expression (5) shows that the decrease of the saturation current comes from the variation of the saturation velocity but also from the variation of the low field mobility, contact resistances and sheet carrier density. Thus the current behaviour depends on parameters located at different positions inside the device. Due to both spatial and temporal dependencies of the temperature, the different parts of the device are not at the same temperature. With thermal simulations we can calculate thermal resistance of these key parts (i.e. in the contact area, access area, near the Schottky contact and at the maximum field location). These dependencies can be then coupled with the analytical electrical model and used to fit the experimental values.

The saturation currents were experimentally determined in this work using 100 ns pulse with 0.1% duty cycle at Vgs=0V and Vds=16V for case temperature of 66 up to 182 °C and for Vds=16V and Vgs of –1V up to –4V for room temperature.

We found for the constant A present in expression (3) a value of 0.2 ± 0.1. This value corresponds to a decrease of $10 \pm 5\%$ for a temperature increase of 150°C. That is in agreement with the predictions obtained by Monte Carlo simulations [3-4,15]. For the saturation velocity we found room temperature value of $10^7 \pm 10^6$ cm/s which is in agreement with f_t measurement (around 17 GHz for this structure and polarisation condition). We deduced a temperature decrease for the saturation velocity near $7x10^3$ cms^{-1}/°C similar to the value predicted by [15].

In order to confirm this result we made measurements on a 2 µm TLM geometry. The measurements were made with both short pulse length (1 µs) and short duty cycle (0.1 %). Thus we avoid excessive heating of the sample. For the estimation of the velocity we suppose that no carrier density gradient exist along the channel. This ensures that the electric field is independent of the position between the contact.

Then for each (I, U) couple of current/voltage value, we can plot the corresponding v[F] characteristic by calculating $v=I/(q\ n_s\ z_g)$ and $F=V/d_{TLM}$ associated expressions, where d_{TLM} is the distance between the contact and z_g is the width of the test sample.

The figure 7 shows clearly no evidence of overshoot effect and a considerable reduction of the saturation velocity in comparison with the bulk value (around 9 10^6 cm/s instead 2 10^7 cm/s as expected from theoretical estimation).

This curve can be fitted by a relationship similar to silicon's velocity-field characteristic i.e:

$$v[F] = \frac{\mu_0\times F}{\left(\left(\frac{\mu_0\times F}{v_{sat}}\right)^{\beta}+1\right)^{1/\beta}};$$

$$\mu_0 = 1000\ cm^2/Vs - v_{sat} = 9.3\ 10^6\ cm/s - \beta = 2.1 \quad (7)$$

To estimate the impact of temperature on this measurement we did compute the temperature rise as a function of the electric field, i.e. the dissipated power. We observed that the temperature elevation associated to the field at which the electron velocity saturate (20 kV/cm) is only 20°C. Therefore we believe that the thermal heating cannot explain the observed saturation.

This result justifies the previous Si-like approach and indicates that the saturation velocity is smaller than theoretical predicted values.

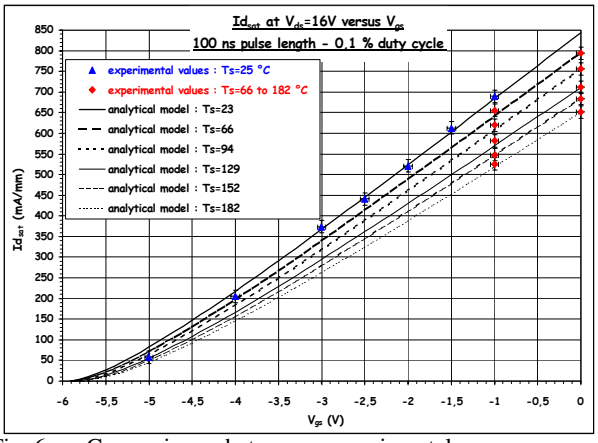

Fig. 6. Comparison between experimental measure and analytical model.

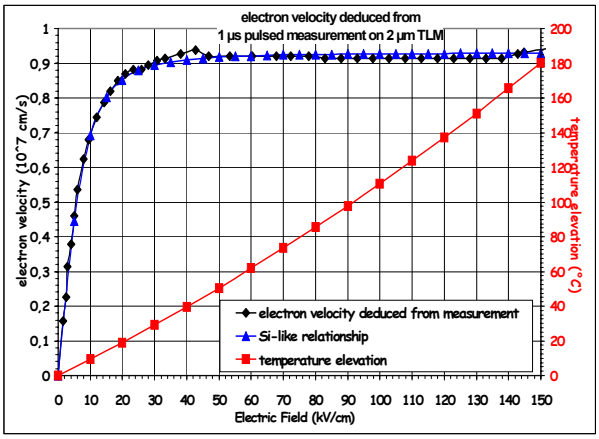

Fig. 7. Velocity field relationship deduced from pulsed 1µs and 0.1 % duty cycle measurements made on a 2 µm TLM.

V. CONCLUSION

Our work coupling experimental results and simulation allows us to estimate the GaN saturation velocity to be about twice lower (10^7 cm/s) than expected in literature. This will impact directly on f_t that will be also twice lower than predicted. On the other hand the temperature variation of v_{sat} are three times lower than for GaAs [13,16]. We expect then more stable temperature operation for the intrinsic GaN device. Nevertheless access resistances of the component have to be considered. In this experiment half of the decrease of the current saturation with temperature arises from the variation of the saturation velocity the other one being linked to the thermal variation of the access resistances. These results were obtained for a 100 ns pulse length for which contact resistance is not heated and channel resistance temperature is not stabilised. Thus for longer pulse duration we expect more pronounced variations of the saturation current with the dissipated power. Then the current decrease of GaN HEMT device will be mainly related to the increase of both channel and contact resistances with temperature, leading to the progressive pinch-off of the component.

ACKNOWLEDGEMENT

The authors wish to acknowledge the support of the French DGA/STTC in the frame of the contract 01.34.050. We do thank our colleagues from TIGER for all the discussions we carried out along.

REFERENCES

[1] N. Fitzer, A. Kuligk, R. Redmer, M. Städele, S. M. Goodnick and W. Schattle "Full band Monte Carlo simulations of high-field electron transport in wide band-gap semiconductors" *Semicond. Sci. Technol.*, vol. 19, pp. S206-S208, (2004).

[2] M. Farahmand, C. Garetto, E. Belloti, K. F. Brennan, M. Goano, E. Ghillino, G. Ghione, J.D. Albrecht and P.P Ruden "Monte Carlo simulations of electron transport in the III-Nitride Wurtzite phase materials system: Binaries and Ternaries" *IEEE Trans. Electron Devices*, vol. 48, p. 535, (2001).

[3] J.D. Albrecht,,R.P. Wang, P.P Ruden, M. Farahmand and K.F. Brennan "Electron transport characteristics of GaN for high temperature device modelling" J. Appl. Phys., vol. 83, p. 4777, (1998).

[4] Udayan V. Bhapkar, M.S. Shur "Monte Carlo calculation of velocity-field characteristics of Wurtzite GaN " J. Appl. Phys., vol. 82, p. 1649, (1997).

[5] F. Dessenne and al., Material Science Eng. vol. 50, p. 315, (1997).

[6] M. Wraback, H. Shen, J.C. Carrano, T. Li, J.C. Campbell, M.J. Shurmann and I.T. Ferguson "Time-resolved electroabsorption measurement of the electron velocity-field characteristic in GaN" *Appl. Phys. Lett.*, vol. 76, p. 1155, (2000).

[7] T.S Yu and F.K. Brennan, "Monte Carlo calculation of two-dimensional electron dynamics in GaN-AlGaN heterostructures " J. Appl. Phys., vol. 91, p. 3730, (2002).

[8] J. Deng, R. Gaska, M.S. Shur, A. Khan, J.W.Yang,, "Negative differential conductivity in AlGaN/GaN HEMTs: real space charge transfer from 2D to 3D states",MIJ-NSR vol. 5S1, Art.W

[9] S. Gokden, N. Balkan and B.K. Ridley "Effect of non-drifting hot phonons on high-field drift velocity in GaN/AlGaN" *Semicond. Sci. Technol.*, vol. 18, pp. 206-211, (2003).

[10] M. Ramonas and A. Matulionis "Monte Carlo simulation of hot-phonon effects in a biased AlGaN/GaN channel" *Semicond. Sci. Technol.*, vol. 19, pp. S424-S426, (2004).

[11] F.N. Trofimenkoff, "Field-dependent mobility analysis of the field-effect transistor", Proc. *IEEE,* vol. 53, p. 1765, (Nov. 1965).

[12] T.Li, Ravindra, P. Joshi and R.D del Rosario, "Requirements for low intermodulation distortion in GaN-$Al_xGa_{1-x}N$ high electron mobility transistors: A model assessment", Proc. *IEEE,* vol. 53, p. 1765, (Nov. 1965).

[13] R. Quay, C. Moglestue, V. Palankovski and S. Selberherr, "A temperature dependent model for the saturation velocity in semiconductor materials" *Mater. Sci. Semicond. Process.*, vol.3, pp. 149-155, (2000).

[14] Mukunda B. Das, "HEMT Device Physics and Models" in *HEMTs and HBTs Devices, Fabrication, and Circuits*, pp. 1-31.

[15] A.F.M.. Anwar, S. Wu and R.T. Webster, "Temperature dependent transport properties in GaN, $Al_xGa_{1-x}N$ and $In_xGa_{1-x}N$ semiconductors" *IEEE Trans. Electron Devices*, vol. 48, p. 567, (2001).

[16] M.J. Littlejohn, J.R. Hauser and T.H. Glisson, "Velocity-field characteristics of GaAs with $_6$-L_6-X_6 conduction band ordering" *J. Applied Physics*, vol. 48, p. 4587, (1977).